Ph.D. Thesis

Immunohistochemical investigations of the neuronal changes induced by chronic recurrent seizures in a pilocarpine rodent model of temporal lobe epilepsy

Norbert Károly M.Sc.

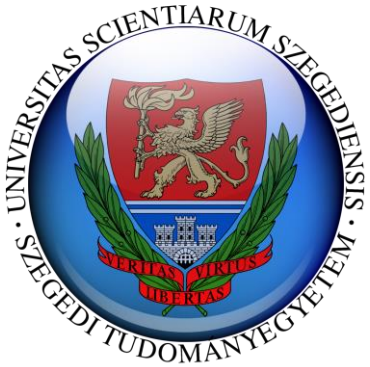

Department of Anatomy, Histology and Embryology
Faculty of Medicine
University of Szeged

Szeged

2017

Ph.D. Thesis

Immunohistochemical investigations of the neuronal changes induced by chronic recurrent seizures in a pilocarpine rodent model of temporal lobe epilepsy

Norbert Károly M.Sc.

Experimental and Clinical Neuroscience Doctoral Programme
Doctoral School of Theoretical Medicine

Supervisors: Endre Dobó M.Sc., Ph.D.; András Mihály, M.D., PhD., D.Sc.

Department of Anatomy, Histology and Embryology
Faculty of Medicine
University of Szeged

Szeged
2017

Abbreviations

CGRP: calcitonin gene-related peptide

CR: calretinin

DAB: diaminobenzidine

DG: dentate gyrus

GC: granule cell

GAP-43: growth-associated phosphoprotein

GluA: AMPA ionotropic glutamate receptor

GluK: kainate ionotropic glutamate receptor

GluN: NMDA ionotropic glutamate receptor

iGluR: ionotropic glutamate receptor

IML: internal molecular layer

IR: immunoreactive

MC: mossy cell

MF: mossy fibre

MFS: mossy fibre sprouting

ML: molecular layer

NeuN: neuronal nuclear protein

NPY: neuropeptide-Y

PB: phosphate buffer

PC: pyramidal cell

PILO: pilocarpine

SE: status epilepticus

SGL: supragranular layer

SL: stratum lucidum

SLM: stratum lacunosum-moleculare

SRS: spontaneous recurrent seizures

Syn-I: synapsin-I

INTRODUCTION, GOALS

Some neuropathological hallmarks of human temporal lobe epilepsy can be produced in rodents by a single injection of pilocarpine (PILO), a muscarinergic agonist. This treatment induces status epilepticus (SE) in the animals within half an hour and induces robust convulsions in the animals acutely, which may display spontaneous recurrent seizures (SRS) after a latent period.

Variable degrees of loss of the principal neurons, such as the pyramidal cells (PCs), mossy cells (MCs) were found in the treated murine hippocampi, A relatively wide layer in the CA areas of the hippocampus is filled with densely packed PCs which form important projections to other brain areas. The loss of these cells is characteristic neuropathological symptom in the epileptogenesis. Evaluation of the degree of damage to the PCs is often made by the neuronal nuclear protein (NeuN) antigene.

The MC is the second type of the principal cells in the hippocampus, with important connections, which can be also vulnerable in different degrees in the epileptic murine species. In mice, calretinin (CR) and GluA2 receptor subunit, whereas in rats, calcitonin gene-related peptide (CGRP) have been reported to be reliable immunhistochemical markers. If these proteins have specific synapse-related functions, any change in the density of these synaptic markers in the internal molecular layer (IML) may reflect the activities of the MCs.

The GCs and their unmyelinated axons, which called mossy fibers (MFs), forming glutamatergic synapses with the MCs, GABAergic interneurones and the PCs in the CA3 area. Those epileptic animals which exhibit SRS are supposed to show intense and ectopic MFS into the supragranular layer (SGL) of the IML which is detectable with the Timm’s silver-sulphide method.

Numerous types of interneurones have been identified in the hippocampus. Many of these neurones can be identified on the basis of the preferred synaptic targets of their axons. Most of these cells are GABAergic, but they are often capable to release neuroactive peptides, as well. One of these

neuromodulators is the neuropeptide-Y (NPY). The expression of NPY increases dramatically in the interneurones of the dentate gyrus (DG) after seizures. The elevated level of NPY has become a useful immunohistochemical marker of epileptic activity in the DG.

The neuronal cell loss due to epileptic activity inevitably induces synaptic reorganization, which includes vacation of postsynaptic sites and axonal sprouting. The density of the synapses can be revealed by visualization of marker proteins, which are known to be present in both the excitatory and inhibitory synapses. One of the general protein constituents of the active synapses is synapsin I (Syn-I). Immunohistochemistry for Syn-I can be readily applied to evaluate the gross changes in the synaptic densities during the axon terminal degeneration and the synaptic reorganization.

Those GCs which lose synaptic inputs in epileptic brains are supposed to release growth factors to trigger axonal sprouting and to regain lost synaptic contacts. A widely used marker protein of the axonal growth is growth-associated phosphoprotein (GAP-43) therefore this marker is suitable to show axonal regeneration and reorganisation, such as MFS.

A possible correlation between the MFS and the other neuronal changes in the PILO-treated animals has been suggested. Direct evidence for this correlation was not available, because the zinc-histochemistry and the classical immunohistochemical methods were not used on tissues from the same animal.

The hippocampal principal neurones are glutamatergic. The vast majority of the hippocampopetal fibres, which derives from the entorhinal cortex predominantly via the perforant and temporoammonic pathways is also glutamatergic. The discrepancies between the responses of the animals to convulsants may be based on the amount and/or the composition of the functional ionotropic glutamate receptors (iGluRs). Since previous studies failed to find explanation for strain differences at the hippocampal receptor level, in the present experiments, we performed a detailed layer-to-layer

analysis in order to reveal the possible strain-dependent differences in the densities of the iGluRs.

In our work, we treated rats and three mouse strains with PILO systemically. The animals exhibiting intense convulsions for at least 30 min were sacrificed after 2-6 months survival periods for comparative morphological studies, which also included a novel combination of immunohistochemistry and the Timm's zinc staining method.

We sought answers for the following questions:

(1) Are there important interspecies differences in the epileptogenic processes in the rodent PILO model?

(2) What are the major interstrain neuropathological differences in the mice, which may account for the different susceptibilities of the strains to the convulsants?

(3) How do the densities of the hippocampal iGluR subunits change in the epileptic mice?

(4) Which are the most beneficial histological methods to confirm the epileptogenesis in the individual animals?

MATERIALS AND METODS

Animal treatment with PILO

Male Wistar rats (220-300 g) and male CFLP, Balb/c and NMRI mice (25-30 g) were used in this study. The animals were injected intraperitoneally with doses of PILO that were suitably adjusted for the species and strains. In preliminary experiments, doses of 380, 190, 180 and 195 mg/kg PILO were found to be appropriate for Wistar rats, CFLP, Balb/c and NMRI mice, respectively.

The animals displayed various levels of salivation and convulsions. With these PILO doses, approximately half of the animals that exhibited SE died on the day of treatment. Ninety minutes after SE onset, the animals were injected with diazepam (Seduxen). The control animals received the same volume of

physiological saline, the solvent of PILO. The animals that developed SE during the treatment were studied, and are referred to below as PILO-treated animals.

Surgical procedure for fornix lesion

A fimbria-fornix lesion was produced in 8 mice anaesthetized intraperitoneally with sodium pentobarbital. The mice were mounted in a stereotaxic apparatus. An L-shaped wire knife (0.7 mm wide) was introduced into the brain through a small hole in the skull, 0.25 mm laterally to the midline and 0.1 mm caudally to the bregma, down to 3.5 mm below the dura. The wire knife was rotated to a distance of 0.25 mm in both directions to produce a lesion of the fornix.

Tissue preparation

The PILO-treated and control animals were sacrificed 2 months after the injections. The animals were deeply anaesthetized with diethyl ether, and perfused through the ascending aorta with sodium sulphide in phosphate buffer (PB), and then with 4% formaldehyde in PB. The brains were dissected and cryoprotected overnight in sucrose in PB. Coronal plane brain sections were cut on a freezing microtome at a thickness of 24 µm on the subsequent days following fixation. The sections, which were devoted for immunohistochemistry, were stored in PB containing sodium azide until processing, while the sections for the Timm's silver sulphide staining were mounted on glass slides, air-dried and stored in dark at ambient temperature until development.

Immunohistochemistry

The sections were treated with 0.5% Triton X-100 and 3% hydrogen peroxide in 0.1 M Tris-HCl; pH 7.6 (TB), and then with normal swine serum (1/10). The following primary antisera were used: rabbit anti-Syn-I (1/1000), sheep anti-NPY (1/48000), goat anti-CR (1/2000), rabbit anti-CGRP (1/10000), mouse

anti-GAP-43 (1/1000), mouse anti-NeuN (1/8000), rabbit anti-GluA1 (1/500), rabbit anti-GluA2 (1/200), rabbit anti-GluA2/3 (1/400); monoclonal rabbit anti-GluK2 (1/3000) and mouse anti-NMDAR1 (1/5000).

The sections were incubated under continuous agitation at room temperature overnight. After washing, the sections were incubated with the appropriate biotinylated secondary antibody (1/500) for 90 min, and finally with peroxidase-labelled streptavidin (1/1000) for 90 min. The sites of immunoreaction were visualized with 3,3’-diaminobenzidine (DAB).

Timm's silver sulphide method

The composition of the staining solution: 60 ml of 50% gum arabic, 10 ml of 2 M sodium citrate buffer (pH 3.7), 30 ml of 5.67% hydroquinone, and 0.5 ml of 17% silver nitrate solution. The sections were continuously agitated in a dark chamber for 50-60 min. The staining process was terminated with 2% sodium acetate, and the unreacted silver ions were removed with 5% sodium thiosulphate. The sections were covered with DPX mounting medium.

Visualization of the fornix lesion

The correct site of the lesion was confirmed via the appearance of erythrocytes extravasated from the breached blood vessels, which exhibited peroxidase-like activity. Their location was revealed by means of the brown colour of the reaction product of 0.05% DAB with 0.01% hydrogen peroxide in PB for 30 min. Thereafter, the sections were stained blue with haematoxylin for Nissl substance.

Image analysis

Pictures were taken with an image-capture system. Image analysis was performed with Adobe Photoshop 7. The pixel density of immunoreactivity was measured by a researcher blind to the experimental conditions of the animals.

Differences between the corresponding hippocampal regions of PILO-treated and control animals were assessed by using the unpaired one-tailed Student's *t* test. Data were analysed and plotted with the aid of GraphPad 4.0 For every measurement. Pearson's correlation analyses were used to evaluate the relationship between the optical densities of NPY and Syn-I.

RESULTS

Mossy fibre sprouting

Timm's staining showed the highest density of strongly stained varicose axons in the hilum and in the stratum lucidum (SL) in both rodents. The animals, which showed SE were checked for the development of the MFs. 40% of the PILO-treated rats and 56% of the PILO-treated mice exhibited massive increase of staining intensity in the hilum and the SL. Moreover, dark zinc-containing varicose axons appeared within a narrow band adjacent to the GCs, ie. the supragranular layer (SGL), which were interpreted as ectopic MFs.

In the reacted rat, in that part of the IML, which was beyond the SGL, the zinc-positive elements disappeared.

In contrast, in the reacted mice, despite the presence of ectopic MFs in the SGL, the homogeneous staining of the IML did not vanish. The fornix lesion did not change the staining pattern and the intensity of the zinc histochemistry of the mouse hippocampus.

Syn-I immunohistochemistry

Strong immunoreactivity for Syn-I was found in the mossy fibers in both rodents. The cell bodies were not labeled. The molecular layer was moderately positive.

In the mouse, PILO treatment did not induce significant alterations in the distribution or density of Syn-I immunoreactivity in the control group. After 2-3 months of survival period, the density of labeled elements in the SL increased

significantly. Moreover, the layer displaying Syn-I immunostaining thickened considerably. The dentate hilum, which contains strongly-stained mossy fiber terminals, as verified by the Timm's staining, displayed a highly significant drop in Syn-I staining intensity. In the IML, the overall staining did not change significantly. Nevertheless, an extra Syn-I immunoreactive band appeared in the IML, in the SGL.

In the rat, Analysis of the brain sections from PILO-reacted and control animals showed similarities and differences as to the mouse. PILO-induced seizures enhanced Syn-I immunoreactivity in every layer, significantly, including the hilum, which contained much weaker immunolabeling in the mouse. The staining pattern in the PILO-reacted rat resembled that of Timm's staining, indicating that sprouted mossy fibers accumulated this synaptic marker protein.

Gap-43 immunohistochemistry

In control animals, the hippocampal GAP-43 immunostaining was similar in the two rodent species. The most intense immunoreactivity was observed in the stratum lacunosum-moleculare (SLM). Somewhat less, but strong and homogeneous staining was found in the IML of the DG in both species. The hilum and the SL of CA3 field were devoid of staining. The principal neurones did not stain.

In the PILO-reacted mouse groups, the staining of the IML was reduced significantly.

In the rat, GAP-43 immunohistochemistry revealed significant reduction in the staining intensity of the IML. In contrast to the mouse, the IML of the rat was not a homogeneously stained band, rather it displayed a middle sublayer, where the GAP-43 immunoreactivity was reduced.

NPY immunohistochemistry

In the PILO-reacted mice the treatment dramatically enhanced the NPY immunoreactivity in the entire DG and the SL. The vast majority of the staining may be attributable to the MFs within both the hilum and the SL. In the molecular layer (ML), the immunoreactivity for NPY was also increased, but yet to much lesser extent than the areas of MFs. Characteristically, one band that seemed slightly more narrow than the inner third of the ML, i.e. the SGL. The strong staining often concealed the NPY-IR neurons in the MF-containing areas. However, in those areas where the MFs were not present, the NPY-IR perikarya were labeled much more intensely than those in the control mice.

The treatment with PILO resulted in similar changes in the rat hippocampus than in that of the mouse. The application of NPY antibodies sharply demarcated the MF-containing hilum and SL. In addition, the SGL was also revealed by NPY immunohistochemistry.

Correlation analysis between NPY and Syn-I immunoreactivities

Because the PILO treatment changed the NPY and Syn-I immunoreactivities in the same layers in both species, possible correlation between these elevated densities were probed in the affected areas in the individual animals. The data for semiquantitative analyses were collected from paired of adjacent sections, the members of which were immunostained for NPY and Syn-I, respectively.

In the mouse, Positive correlations were found between the two markers in the SL. The increased density of the NPY immunoreactivity was inversely proportional to the density of Syn-I in the hilum.

In the rat, positive proportional changes were found between the markers in the SL. The density of the NPY immunoreactivity in the hilum, in contrast to the mice, was directly proportional to the Syn-I.

Effects of seizures on principal neurons

Mouse mossy cells

Two immunohistochemical markers (CR and GluA2/3 subunit) have been used for the detection of the mouse MCs. CR-IR somata and processes were seen in the DG, and a prominent IR band was observed in the IML.

The densities of CR-IR cells were compared in the control and PILO-reacted CFLP strain. Representative sections were counterstained with cresyl violet for cell nuclei and Nissl substance. None of the counterstained sections showed noticeable cell loss in the DG in convulsing animals.

CR immunoreactivity in the IML did not change after PILO treatment. Since some authors have postulated that a considerable number of the CR-IR processes in the IML originate from the supramamillary nucleus through the fornix, this bundle of fibres was transected in 4 control animals, in order to evaluate the proportions of the CR-IR synapses of the extra- and intrahippocampal sources. We found that fornix transection did not cause changes in the CR-IR pattern in the hilum.

The perikarya of the MCs were also verified by GluA2/3 antibodies in the Balb/c and NMRI mice. PILO-treatment resulted in significant changes in the immunoreactivity for this AMPA subunit in the hilum. The density of the MCs was reduced in both mouse strains significantly.

Rat mossy cells

CGRP immunoreactivity was used in rats to mark the MCs and their projections. In the control animals, the most intense staining was found in the IML, which appeared as a homogeneous band. In addition, various number of weakly stained CGRP immunoreactive multipolar neurons were also scattered in the hilum. Labeled neuronal elements were not found beside the DG.

The PILO treatment resulted in marked changes in the CGRP immunoreactivity. Principally, the staining disappeared from the IML in each animal. CGRP-IR

hilar neurons were only occasionally found, or no cells per section could be seen.

Effects of convulsions on the pyramidal cells

Neuronal loss was evaluated by means of NeuN immunostaining in the PILO-responsive animals. No changes was found in the number of PCs in the Wistar rat and CFLP mice but noticeable reductions were found int he number of these cells of the Balb/c and NMRI strains in the CA3a and CA3b subregions.

In the NMRI strain, the cell loss was more pronounced, 8 out of the 18 PILO-responsive mice displayed patchy neuronal loss in the PC layer of CA1 and CA3 regions. Beside the loss of CA3 PCs, the superior blade of the GC layer was damaged to a large extent in the sclerotic mice.

Changes of the iGluRs in the Balb/c and NMRI mice

AMPA receptor subunits

The density of the GluA1 immunoreactivity decreased in every hippocampal layer, except the stratum radiatum of CA1 of the NMRI mice. In all other layers, very similar changes were observed in both strains. The most significant reductions were found in the dentate hilum in the Balb/c and NMRI mice.

The GluA2 immunoreactivity decreased in both strains. The highest reduction of the GluA2 immunoreactivity was found in the synaptic field of the MFs in both strains. The statistical analysis of the GluA2/3 immunohistochemical results showed largely similar alterations. The lowest density values and the highest degree of reduction of the optical densities were found in the hilum in the Balb/c and NMRI mice and the optical density of the hilar immunopositive neurones was reduced significantly in both strains as well.

NMDA receptor subunits

PILO treatment exerted measurable effects on the GluN1 immunostaining in the hippocampal layers of the two examined mouse strains. In the Balb/c animals, the intensity of the staining in the stratum radiatum and in the SLM of CA1 were significantly decreased. The PILO treatment did not cause modification in the immunostaining density of the overall ML of the DG. However, in the close vicinity of the GC layer, that is in the SGL, our semiquantitative method revealed a significant intensity decrease (-16%). In the NMRI mice the only significant change was an increase (+29%), measured in the SLM of CA1.

Kainate receptor subunits

The application of the low affinity GluK2 kainate receptor subunit resulted in a staining pattern, which was very similar to that of the AMPAR antibodies in the hippocampus. In the control animals, weak immunostaining was found in the pyramidal and the granular layers, in the hilum and in the SL of CA3. The layer-to-layer comparisons of the data from the Balb/c and NMRI strains revealed significant intensity differences in the GluK2 immunoreactivities: the ML and the hilum of the NMRI strain exhibited higher density values than those in the Balb/c mice.

After PILO treatment, the intensity of the GluK2 immunoreactivity increased in the hippocampus. The highest increase was observed in the hilum of the Balb/c mice, while opposite alteration was observed of the GluK2 density in this region of the NMRI mice. Intensity increases were also significant in the stratum radiatum of CA1 and the SLM of CA3 in the Balb/c strain while less increase was observed in those layers of the NMRI mice. The ML of the Balb/c mice showed intensity increase, while no alteration was measured in the ML of the NMRI mice.

CONCLUSION

In a rodent model of epilepsy, similar treatments of rats and mice with PILO induce comparable behavioural patterns and repeated episodes of chronic spontaneous seizures. The hippocampi of these PILO-treated animals were analysed by means of a novel combination of zinc histochemistry and immunohistochemistry for certain neuronal markers.

(1) Important interspecies differences were found during the epileptogeneses of the rat and the mouse in the PILO model.

(a) The hilar MCs are more vulnerable in rats than in mice.

(b) The higher damage is accompanied by the more intense ectopic sprouting of the GCs.

(2) Differences in predispositions to PILO-induced neuronal alterations were found in mouse strains.

(a) The MCs of the CFLP seemed to resist the effect of PILO, whereas these cells of NMRI mice were found to be highly susceptible to the same treatment.

(b) A remarkably lower density of the calcium impermeable GluA2 subunit was revealed in hilum of the NMRI than of the Balb/c mice.

(3) PILO-induced chronic seizures resulted in significant alterations of the patterns of the iGluR subunits in mouse strains.

(a) The NPY immunoreactivity was increased proportionally to the decrease of the immunoreactivity of GluA1.

(b) The more the immunoreactivity for NPY was increased, the less the GluA2 immunoreactivity was reduced.

(4) Our collated results showed that NPY immunohistochemistry may be the most sensitive and reliable for visualisation of the epileptic processes in each tested murine strains.

LIST OF PUBLICATIONS RELATED TO THE THESIS

I. **Karoly N**, Mihaly A, Dobo E (2011) Comparative immunohistochemistry of synaptic markers in the rodent hippocampus in pilocarpine epilepsy. Acta Histochem 113:656-662.

II. **Karoly N**, Dobo E, Mihaly A (2015) Comparative immunohistochemical study of the effects of pilocarpine on the mossy cells, mossy fibres and inhibitory neurones in murine dentate gyrus. Acta Neurobiol Exp 75(2):220-237.

III. Dobo E, Torok I, Mihaly A, **Karoly N**, Krisztin-Peva B (2015) Interstrain differences of ionotropic glutamate receptor subunits in the hippocampus and induction of hippocampal sclerosis with pilocarpine in mice. J Chem Neuroanat 64-65:1-11.